PHYSICAL REVIEW LETTERS

Real-Time Observation of Phase-Controlled Molecular Wave-Packet Interference

Kenji Ohmori,[1,2,3,4,*] Hiroyuki Katsuki,[1,2,4] Hisashi Chiba,[1,3,4] Masahiro Honda,[3,4] Yusuke Hagihara,[3,4]
Katsutoshi Fujiwara,[3] Yukinori Sato,[3,4] and Kiyoshi Ueda[3,4]

[1]*Institute for Molecular Science, National Institutes of Natural Sciences, Myodaiji, Okazaki 444-8585, Japan*
[2]*The Graduate University for Advanced Studies (SOKENDAI), Myodaiji, Okazaki 444-8585, Japan*
[3]*IMRAM, Tohoku University, Katahira 2-1-1, Sendai 980-8577, Japan*
[4]*CREST, Japan Science and Technology Agency, Kawaguchi, Saitama 332-0012, Japan*

The quantum interference of two molecular wave packets has been precisely controlled in the B electronic state of the I_2 molecule by using a pair of fs laser pulses whose relative phase is locked within the attosecond time scale and its real-time evolution has been observed by another fs laser pulse. It is clearly observed that the temporal evolution changes drastically as a function of the relative phase between the locked pulses, allowing us to read both amplitude and phase information stored in the wave functions of the molecular ensemble.

Wave-packet (WP) interferometry is a clear manifestation of wave nature of matter. It is also a basic scheme of controlling a variety of quantum systems with possible applications to novel quantum technologies such as bond-selective chemistry and quantum computation. The WP interferometry has so far been developed with electronic WP's in atoms [1–7] and vibrational WP's in molecules [8–12], based on the measurement of population of the excited state sensitive to the relative phase of the twin optical pulses that produce a pair of WP's. The phase dependence of the population is often described in terms of spectral interference of the twin pulses that can be observed when they are frequency dispersed with a grating to be temporally overlapped with each other: the population of each eigenstate within a WP is linearly dependent on the intensity of its resonant frequency component within the twin pulse spectrum. Such correspondence is, however, plausible only in the limit of the linear-response regime [11], and is usually distorted by statistical dephasing or decoherence [8–10,12] that happens between the twin pulses. Moreover, population is the modulus square of a wave function, so that it does not contain phase information in itself. It is thus necessary to observe and interpret WP interference in terms of the time-domain picture. In this Letter, we will demonstrate a real-time observation of the quantum interference of two molecular WP's tightly phase locked on the attosecond time scale. The temporal evolution of WP interference gives additional important information on the relative phase of the eigenstates within the controlled WP. This kind of phase information was unknown in our previous population measurements of the eigenstates [11]. Reading both phase and amplitude information is indispensable for developing novel quantum technologies such as atom- and molecule-based information processing [3,13].

Figure 1 illustrates our pump-control-probe scheme, and the experimental system is similar to that used in our previous WP interferometry with HgAr dimers [11]. However

the apparatus was newly constructed. Briefly, a fs probe laser pulse was incorporated in combination with the ns probe laser pulse; the continuous molecular jet source was employed instead of the previous pulsed one; a 1 kHz laser system was employed instead of the previous 10 Hz system [14]; and a feedback control was newly incorporated for the long-time stabilization of the relative phase $\theta_{\text{p-c}}$ of the pump and control pulses. The I_2 molecules were prepared in the electronic ground state ($X^1\Sigma_g^+$) by an expansion of heated I_2/Ar mixture (∼320 K, ∼1 atm) into a vacuum chamber through a nozzle. The output of a Ti:sapphire laser system (pulse width: ∼100 fs, repetition rate: 1 kHz; Quantronix) was used to pump two optical parametric amplifiers (OPA) (Quantronix). The outputs of those two OPA's were tuned, respectively, to ∼612 and ∼396 nm. The 612 nm pulse (bandwidth: ∼200 cm^{-1}, pulse width: ∼100 fs) was input to an attosecond phase modulator (APM) [11]. APM is a Michelson type interferometer highly stabilized in a vacuum chamber to generate a phased pair of laser pulses, which were used as the pump
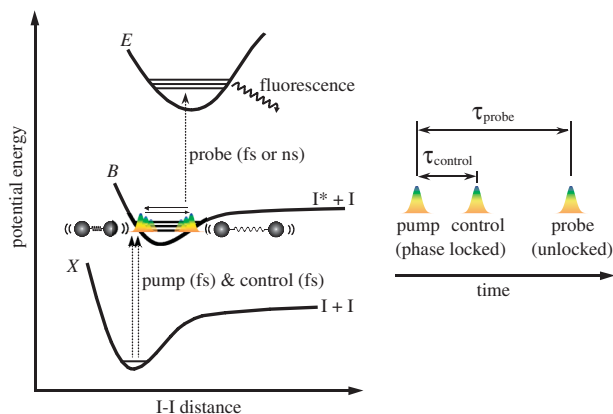

FIG. 1 (color online). Pump-control-probe scheme for the real-time or state-resolved measurement of wave-packet interference with the fs or ns probe pulse. The potentials are only schematic.

and control pulses. One arm of APM has a mechanical translation stage for coarse setting of the delay $\tau_{control}$ between the pump and control pulses, and the other arm has a gas cell for the pressure scan of $\tau_{control}$ with atto-second resolution. The pump and control pulses were directed collinearly into the vacuum chamber to intersect the molecular jet. The vibrational eigenstates around $\nu_B = 7$–13 of the B state were mainly excited, and two molecular WP's were created sequentially around the inner turning point of the potential curve. The 396 nm pulse (bandwidth: ~ 150 cm^{-1}) was used for real-time laser-induced fluorescence spectroscopy measurements of the WP amplitude within the Franck-Condon (FC) window of the E-B transition opened by this probe pulse [15,16]. The present FC window is estimated to be around the outer classical turning points of $\nu_B = 9$ and 10. The delay τ_{probe} of this probe pulse was tuned by another mechanical stage with a resolution of about 13 fs. A narrow band ns probe pulse produced by an Excimer-pumped dye laser (Lambda Physik, SCANMATE 2E) was also used to measure the population of a particular vibrational eigenstate within WP's with its delay τ_{probe} fixed to ~ 35 ns ($\pm \sim 5$ ns jitter) from the pump and control pulses. With this system we made two different types of measurements of WP interference. First, we used the ns probe pulse and scanned its wavelength around 389–391 nm to measure the E-B excitation spectrum with a fixed $\tau_{control}$, which has been done previously for the HgAr dimers [11]. This measurement retrieves the population ratio among the vibrational eigenstates, which we call a "population code," involved in the WP's. Second, we used the fs probe pulse and scanned its delay τ_{probe} using the mechanical stage with a fixed $\tau_{control}$ to observe temporal evolution of the WP interference [17]. The cross correlation of the pump and probe pulses was not taken, and their timing was calibrated by each measured evolution. In both types of measurements, the fixed $\tau_{control}$ was stabilized by periodical passive feedback control of the mechanical stage of APM in every ~ 10 sec with a tolerance of $\sim \pm 40$ asec ($\sim 0.04\pi$ in θ_{p-c}), which is regarded as a typical upper limit of the deviation of $\tau_{control}$ in each measurement.

Apart from these interferometric measurements, we measured the B-X fluorescence excitation spectrum by scanning the wavelength of the ns pulse without shining the pump and control pulses. From these measurements, we estimated the rotational and vibrational temperatures, T_r and T_v, of our ensemble of I_2 to be ~ 20 K and $\sim 220 \pm 40$ K, respectively. As for the population summed over the principal members in the population codes: $\nu_B = 8$–12, the combination of the present T_v, the pump wavelength, and the Franck-Condon factors gives dominant transitions from the vibrational levels $\nu_X = 1$–4 of the X state, which we estimated from the B-X fluorescence excitation spectra measured by scanning the wavelength around 599.0–622.5 nm. The observed signal in the present study was, therefore, the sum of the contributions from different ν_X's

distributed under the present T_v, weighted by the relevant Franck-Condon factors. In all of these estimations based on the B-X fluorescence excitation spectra, we did not take into account vibrational- and rotational-level dependence of the predissociation yield of the B state [18].

First we have carried out a set of measurements with the pump-control delay $\tau_{control} \sim 305$ fs $\cong 1 T_{vib}$, where T_{vib} is a classical vibrational period of I_2. Figure 2 shows two different temporal evolutions of WP interference taken with two different θ_{p-c}'s separated from each other by $\sim \pi$. It is clearly seen from those temporal evolutions in Fig. 2 that the WP is once produced on the B-state potential by the pump pulse, oscillates for one vibrational period, and then interacts with the second WP to give a drastic contrast between constructive and destructive interferences. The ordinary frequency domain interpretation based on the spectral interference of twin pulses may be useful to elucidate population codes [11], but is no longer suitable for this real-time observation. As for the constructive case shown in Fig. 2(a), the control pulse amplifies the beat amplitude by a factor close to 4, indicating that the present control is almost complete. Similar real-time and high-contrast control of an atomic transition was recently performed [19].

Another set of measurements has been made with $\tau_{control} \sim 460$ fs $\cong 1.5 T_{vib}$. Figure 3(a) shows four different population codes taken with four different θ_{p-c}'s spaced in steps of $\sim \pi/2$; they are designated codes A–D. The population code has a clear dependence on θ_{p-c}. Codes A
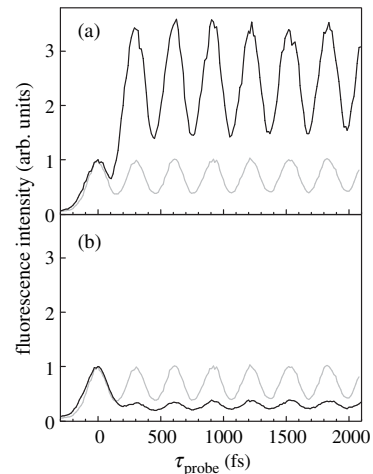

FIG. 2. Real-time evolution of the interference of two phase-locked vibrational wave packets on the B-state potential of the I_2 molecule. The pump and control delay $\tau_{control}$'s are tuned to $\sim 1 T_{vib}$ (~ 305 fs), where T_{vib} is a classical vibrational period of I_2. The relative phase θ_{p-c} of the pump and control pulses is different by $\sim \pi$ between (a) and (b). The shaded trace is the evolution measured without control pulse and is displayed for reference. Each trace is a summation of four repeated scans. The origin of the probe delay ($\tau_{probe} = 0$) denotes a position of the top of the first undulation in each measured trace. The vertical scaling of each trace is arbitrary and is normalized by the height of its first undulation.

and C are, however, similar codes, difficult to distinguish only by the population measurements. Figure 3(b) shows temporal evolutions of WP interference taken with the same $\theta_{p\text{-}c}$'s as for codes A–D; a possible deviation of $\theta_{p\text{-}c}$ in each set is estimated to be less than $\sim 0.06\pi$. The temporal evolution also has a clear dependence on $\theta_{p\text{-}c}$. Similar correspondences between population distributions and wave-packet recurrences have been recently predicted in theoretical simulations [20]. From the present real-time measurements, we have found that similar population codes A and C give distinct quantum beats in antiphase with each other, so that they can be clearly distinguished. Figure 3(c) shows a simulated $\tau_{control}$ dependence of the population n_{ν_B} of $\nu_B = 10$ around $\tau_{control} = 460$ fs. This dependence was calculated in the limit of linear-response regime by [11]

$$n_{\nu_B}(\tau_{control}) = \sum_{\nu_X} C_{\nu_B - \nu_X} \cos^2(\omega_{\nu_B - \nu_X} \tau_{control}/2), \quad (1)$$

where $C_{10-2} = 0.6$ for $\nu_X = 2$, $C_{10-3} = 0.4$ for $\nu_X = 3$, and contributions from other ν_X's were regarded as negligible ($\leq 8\%$). These values of $C_{10-\nu_X}$'s were estimated
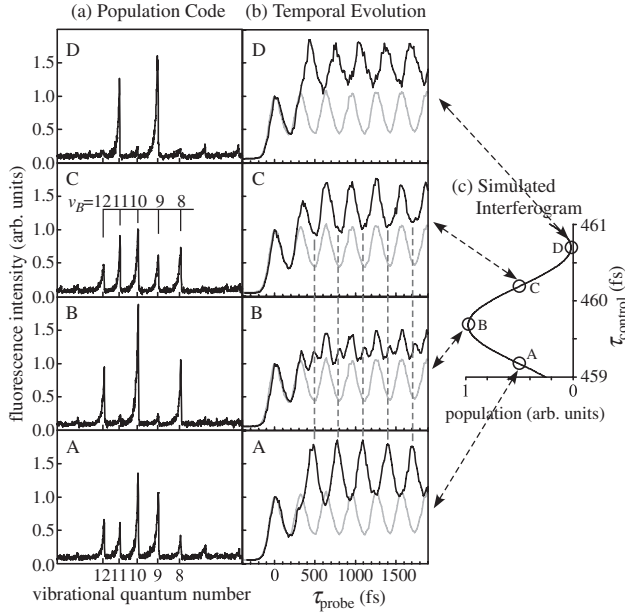

FIG. 3. Wave-packet interference measured and simulated with the pump and control delay $\tau_{control}$ tuned to $\sim 1.5 T_{vib}$ (~ 460 fs), where T_{vib} is a classical vibrational period of I$_2$. (a) *E-B* excitation spectrum, which we call the population code, measured by scanning the wavelength of the ns probe pulse delayed by ~ 35 ns from the pump and control pulses. The relative phase $\theta_{p\text{-}c}$ of the pump and control pulses is increased in steps of $\sim \pi/2$ in going from code A to code D. (b) Real-time evolutions of the wave-packet interference measured with the same $\theta_{p\text{-}c}$'s as for codes A–D. See the caption of Fig. 2 for further details. (c) Simulation of $\tau_{control}$ dependence of the population of $\nu_B = 10$, $n_{10}(\tau_{control})$, calculated from Eq. (1). The arrows stand for approximate correspondences in $\theta_{p\text{-}c}$, and not in the absolute values of $\tau_{control}$.

from the *B-X* excitation spectrum and the power spectrum of the pump pulse. The transition frequencies ω_{10-2} and ω_{10-3} were taken from a previous spectroscopic study [21]. Judging from the $\theta_{p\text{-}c}$ dependence of the peak intensities of $\nu_B = 10$ seen in Fig. 3(a), it is reasonable to consider that $\theta_{p\text{-}c}$'s for codes A–D almost correspond to $\theta_{p\text{-}c}$'s for points A–D in this simulated interferogram shown in Fig. 3(c). After the irradiation of the control pulse, the time-dependent wave function $\psi_{\nu_B - \nu_X}$ of the vibrational level ν_B excited from the level ν_X is written in terms of the eigenfunction $|\nu_B\rangle$ and the transition frequency $\omega_{\nu_B - \nu_X}$ as

$$|\psi_{\nu_B - \nu_X}\rangle = |\nu_B\rangle[\exp(-i\omega_{\nu_B - \nu_X}t) + \exp(-i\omega_{\nu_B - \nu_X}(t - \tau_{control}))], \quad (2)$$

where the intensity difference between the pump and control pulses is considered negligible. The real component of the time-dependent part of Eq. (2),

$$T(t) = \cos(\omega_{\nu_B - \nu_X}t) + \cos[\omega_{\nu_B - \nu_X}(t - \tau_{control})], \quad (3)$$

has been calculated with $\tau_{control}$'s corresponding to points A and C marked in Fig. 3(c) for the initial vibrational levels $\nu_X = 2$ and 3. From the calculated $T(t)$'s shown in Fig. 4, it is seen for each ν_X that the relative quantum phase among different ν_B's within each of the groups of even and odd ν_B's is almost the same between points A and C; each of the even and odd levels are almost in phase for the period around $t = 613$ fs ($\cong 2T_{vib}$), as displayed in Fig. 4. Hence the wave packet arising from one of the initial ν_X's ($=2$ or 3) is approximately described as

$$|\Psi_{B(\nu_X)}\rangle \cong \sum_{\text{even } \nu_B} c_{\nu_B - \nu_X} |\nu_B\rangle \exp(-i\omega_{\nu_B - \nu_X}t')$$
$$+ \sum_{\text{odd } \nu_B} c_{\nu_B - \nu_X} |\nu_B\rangle \exp[-i(\omega_{\nu_B - \nu_X}t' - \delta)], \quad (4)$$

where $t' \sim t - 613$, the amplitudes $c_{\nu_B - \nu_X}$'s are real, and δ represents the relative phase of the odd levels to the even levels. Then it is seen from Fig. 4 that this relative phase δ is shifted by π between points A and C shown in Fig. 3(c), yielding sign reversal ($+ \leftrightarrow -$) of the wave functions of the odd levels, which is, of course, unable to be readout in the population measurements in the frequency domain, where the square of the amplitude of each eigenfunction is measured. The present antiphase beats in Fig. 3(b) observed for codes A and C are thus attributable to this π phase shift between points A and C; these two points, however, give similar codes to be barely distinguishable in the population measurements. The present measurements thus indicate that a combination of the population code and the temporal evolution could retrieve both the phase and amplitude information written in the WP.

Similar efforts to retrieve phase and amplitude information stored in WP's have been made for a Rydberg WP in the Cs atom by measuring a population distribution created by interference with another reference WP [3]. Another
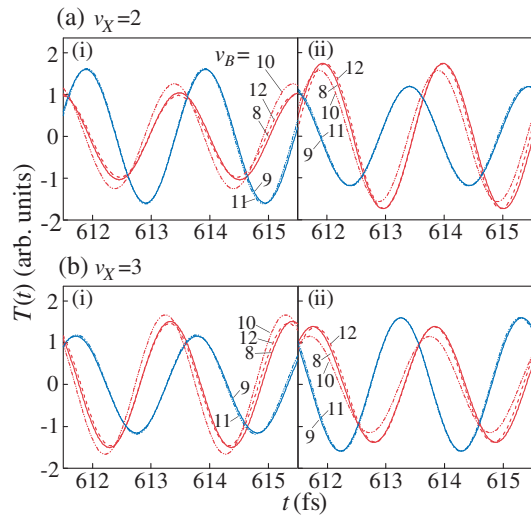
FIG. 4 (color).   The real component of the time-dependent part $T(t)$ of the vibrational wave functions of $\nu_B = 8\text{--}12$ excited from (a) $\nu_X = 2$ and (b) $\nu_X = 3$ simulated by Eq. (3) with (i) $\tau_{\mathrm{control}} = 459.18$ fs and (ii) $\tau_{\mathrm{control}} = 460.19$ fs, which are the pump-control timings corresponding, respectively, to the points A and C marked in the simulated interferogram shown in Fig. 3(c).

similar effort to characterize both momentum and position information of a WP has been made for a vibrational WP in a Na dimer by measuring the time- and frequency-resolved spectrum of spontaneous emission [22]. The combination of a population code and a temporal evolution that we have demonstrated in this Letter can be regarded as another straightforward and robust approach to provide full quantum information of a WP in wide range of quantum systems.

In summary, we have controlled quantum interference of two vibrational WP's in the iodine molecule by using a pair of phase-locked fs pulses, and the real-time evolution of that interference has been observed by another fs probe pulse. The real-time evolution shows a clear dependence on the relative phase $\theta_{\mathrm{p\text{-}c}}$ between the locked pulses highly stabilized on the attosecond time scale. We have also measured a population code, which is a population ratio among the vibrational eigenstates within WP's. The population code also shows a clear dependence on $\theta_{\mathrm{p\text{-}c}}$. The ordinary frequency domain interpretation based on the spectral interference of locked pulses may be useful to elucidate $\theta_{\mathrm{p\text{-}c}}$ dependence of population codes, but is no longer suitable for the present real-time observation. Moreover, the real-time evolution has allowed us to obtain additional phase information unable to be obtained from population codes. The combination of a population code and real-time evolution is useful to obtain both phase and amplitude information stored in a WP, which is indispensable for developing novel quantum technologies such as atom- and molecule-based information processing. All these fea-

tures provides basis for opening new perspective of coherent control in a wide variety of quantum systems.

*Electronic address: ohmori@ims.ac.jp
[1] M. W. Noel and C. R. Stroud, Jr., Phys. Rev. Lett. **75**, 1252 (1995); **77**, 1913 (1996); Opt. Express **1**, 176 (1997).
[2] R. R. Jones *et al.*, Phys. Rev. Lett. **71**, 2575 (1993); R. R. Jones *et al.*, J. Phys. B **28**, L405 (1995); R. R. Jones, Phys. Rev. Lett. **75**, 1491 (1995).
[3] T. C. Weinacht, J. Ahn, and P. H. Bucksbaum, Phys. Rev. Lett. **80**, 5508 (1998); T. C. Weinacht, J. Ahn, and P. H. Bucksbaum, Nature (London) **397**, 233 (1999); J. Ahn, T. C. Weinacht, and P. H. Bucksbaum, Science **287**, 463 (2000).
[4] L. D. Noordam, D. I. Duncan, and T. F. Gallagher, Phys. Rev. A **45**, 4734 (1992); J. F. Christian *et al.*, Opt. Commun. **103**, 79 (1993).
[5] L. Marmet *et al.*, Phys. Rev. Lett. **72**, 3779 (1994).
[6] V. Blanchet *et al.*, Phys. Rev. Lett. **78**, 2716 (1997); M. A. Bouchene *et al.*, Eur. Phys. J. D **2**, 131 (1998).
[7] M. Bellini, A. Bartoli, and T. W. Hänsch, Opt. Lett. **22**, 540 (1997).
[8] N. F. Scherer *et al.*, J. Chem. Phys. **95**, 1487 (1991); **96**, 4180 (1992).
[9] V. Blanchet, M. A. Bouchene, and B. Girard, J. Chem. Phys. **108**, 4862 (1998).
[10] Ch. Warmuth *et al.*, J. Chem. Phys. **112**, 5060 (2000); **114**, 9901 (2001).
[11] K. Ohmori *et al.*, Phys. Rev. Lett. **91**, 243003 (2003).
[12] M. Fushitani *et al.*, Phys. Chem. Chem. Phys. **7**, 3143 (2005).
[13] Z. Amitay, R. Kosloff, and S. R. Leone, Chem. Phys. Lett. **359**, 8 (2002); J. Vala *et al.*, Phys. Rev. A **66**, 062316 (2002).
[14] Y. Sato *et al.*, *Ultrafast Phenomena XIV* (Springer-Verlag, Berlin, 2005), p. 526.
[15] T. Lohmüller *et al.*, J. Chem. Phys. **120**, 10 442 (2004).
[16] H. Katsuki *et al.* (to be published).
[17] The ns and fs probe pulses were tuned to slightly different wavelengths so that the *E*-state vibrational levels accessed by the fs probe pulse are estimated to be lower by 3–4 than those employed in measuring the population code.
[18] See, for example, J. Tellinghuisen, J. Chem. Phys. **57**, 2397 (1972); M. Broyer, J. Vigué, and J. C. Lehmann, J. Chem. Phys. **63**, 5428 (1975); E. A. Pazyuk *et al.*, Mol. Phys. **99**, 91 (2001).
[19] A. Monmayrant, B. Chatel, and B. Girard (to be published).
[20] E. D. Boleat and H. H. Fielding, Mol. Phys. **103**, 491 (2005).
[21] P. Luc, J. Mol. Spectrosc. **80**, 41 (1980).
[22] T. J. Dunn *et al.*, Phys. Rev. Lett. **70**, 3388 (1993); T. J. Dunn, I. A. Walmsley, and S. Mukamel, Phys. Rev. Lett. **74**, 884 (1995).